ARTICLE
Journal of Cellular Biochemistry 107:460–472 (2009)

Journal of Cellular Biochemistry

OxLDL Upregulates Caveolin-1 Expression in Macrophages: Role for Caveolin-1 in the Adhesion of oxLDL-Treated Macrophages to Endothelium

Chau-Chung Wu,[1**] Shu-Huei Wang,[2] I.-I. Kuan,[2] Wei-Kung Tseng,[3] Ming-Fong Chen,[1] Jiahn-Chun Wu,[2] and Yuh-Lien Chen[2*]

[1]*Department of Internal Medicine and Primary Care Medicine, National Taiwan University Hospital, Taipei, Taiwan*
[2]*Department of Anatomy and Cell Biology, College of Medicine, National Taiwan University, Taipei, Taiwan*
[3]*Department of Internal Medicine, E-Da Hospital, Kaohsiung, Taiwan*

ABSTRACT

Caveolin-1, a principle component of caveolae, is present in several cell types known to play an important role in the development of atherosclerosis. In this study, its distribution and expression were studied in the arterial walls of hypercholesterolemic rabbits and apo-E-deficient mice and in oxidized low-density lipoprotein (oxLDL)-treated RAW264.7 macrophages. Immunohistochemical studies showed that staining for caveolin-1 expression was stronger in atherosclerotic lesions in hypercholesterolemic rabbits and apo-E-deficient mice compared to normal rabbits and mice and was closely associated with macrophages. OxLDL treatment increased caveolin-1 protein expression in RAW264.7 macrophages in a time- and dose-dependent manner. The increase in caveolin-1 expression was dependent on phosphorylation of the mitogen-activated protein kinases (MAPKs) extracellular signal-regulated kinase1/2 (ERK1/2), p38, and Jun N-terminal kinase (JNK) and the transcriptional activation and translocation of nuclear factor-κB (NF-κB). OxLDL also induced caveolin-1 mRNA expression and this effect was not seen in the presence of inhibitors for transcription or de novo protein synthesis. OxLDL increased the adhesion of RAW264.7 macrophages to endothelial cells via an increase in caveolin-1 expression, and the adhesion was reduced by the use of anti-caveolin-1 antibody or caveolin-1-specific shRNA. These results show that oxLDL increases caveolin-1 expression in macrophages through the MAPKs/NF-κB pathway. The caveolin-1 levels are closely associated with the adherence of monocytes/macrophages to endothelial cells and their accumulation within the arterial intima after hypercholesterolemia insult, resulting in the progression of atherosclerosis. J. Cell. Biochem. 107: 460–472, 2009.

KEY WORDS: CAVEOLIN-1; HYPERCHOLESTEROLEMIA; oxLDL; MACROPHAGES; MAPKs

The adherence of monocytes to endothelial cells, followed by their transmigration into the subendothelial space and differentiation into macrophages, is a pivotal theme of atherosclerosis. The uptake of excessive amounts of lipoprotein-derived lipids by macrophages leads to their conversion into foam cells [Ross, 1993]. The availability of oxidized low-density lipoprotein (oxLDL) in the subendothelial space and the macrophage-specific expression of scavenger receptors that lack feedback regulation are responsible for the high lipid enrichment of cells [Brown and Goldstein, 1983]. Under physiological conditions, the net accumulation of lipids in the subendothelial space of blood vessels is a result of a complex set of events, including the overall local redox balance

Abbreviations used: AP-1, activation protein-1; BCECF/AM, 2′,7″-*bis*-(2-carboxyethyl)-5-(and -6)-carboxyfluorescein/acetoxymethyl ester; CL, control; EMSA, electrophoretic mobility shift assay; ERK1/2, extracellular signal-regulated kinase 1/2; HUVECs, human umbilical vein endothelial cells; nLDL, native low-density lipoprotein; oxLDL, oxidized low-density lipoprotein; JNK, Jun N-terminal kinase; MAPKs, mitogen-activated protein kinases; MTT, 3-(4,5-dimethylthiazol-2-yl)-2,5-diphenyl tetrazolium bromide; NF-κB, nuclear factor-κB; Pl, parthenolide.

Grant sponsor: National Science Council; Grant numbers: NSC 96-2628-B-002-051-MY3, NSC 96-2314-B-002-150-MY3, NSC 95-2752-B-006-005-PAE, NSC 95-2314-B-002-123.

*Correspondence to: Prof. Dr. Yuh-Lien Chen, Department of Anatomy and Cell Biology, College of Medicine, National Taiwan University, No. 1, Section 1, Ren-Ai Rd, Taipei 100, Taiwan. E-mail: ylchenv@ntu.edu.tw

**Correspondence to: Dr. Chau-Chung Wu, Department of Internal Medicine, National Taiwan University Hospital, No. 7, Chung-Shan S. RD., Taipei 100, Taiwan. E-mail: chauchungwu@ntu.edu.tw

Received 20 August 2008; Accepted 18 February 2009 • DOI 10.1002/jcb.22144 • 2009 Wiley-Liss, Inc.
Published online 23 March 2009 in Wiley InterScience (www.interscience.wiley.com).

and the rate of cholesterol accumulation and its removal via the reverse cholesterol transport pathway [Schroeder et al., 2001]. Caveolin proteins have been implicated in the regulation of cellular cholesterol metabolism and lipid uptake and efflux [Fielding and Fielding, 2001]. Caveolin-1 is the main structural protein of caveolae. The majority of the available information about caveolins comes from studies on fibroblasts and endothelial cells, which are relatively rich in caveolae and express high amounts of caveolin-1 and caveolin-2 [Scherer et al., 1997; Frank et al., 2003]. However, the evidence for caveolin expression in macrophages is conflicting [reviewed in Gargalovic and Dory, 2003].

Caveolin-1 has been suggested to play a critical role in the development of atherosclerosis [Lisanti et al., 1994; Cohen et al., 2004]. Electron microscopic studies have clearly shown that endothelial cell caveolae are involved in the uptake and transcytosis of native (nLDL) and/or oxLDL and in the initiation of atherosclerosis [Vasile et al., 1983; Kim et al., 1994]. We were therefore interested in understanding the mechanism of action of oxLDL on macrophages and determining whether it stimulates or blocks the expression of caveolin-1. The effects of oxLDL on cytokine expression involve the activation of multiple signaling molecules in transduction pathways [Kunsch and Medford, 1999]. Among these, mitogen-activated protein kinases (MAPKs) are highly conserved serine/threonine kinases that are activated in response to a wide variety of stimuli, including growth factors, activation of G protein-coupled receptors, and environmental stresses [Zhao et al., 2002; Xu et al., 2008]. Three major members of the structurally related MAPKs, extracellular signal-regulated kinase 1/2 (ERK1/2), Jun N-terminal kinase (JNK), and p38 MAP kinase, have been identified in mammalian cells. The signals can be transduced to downstream molecules and activate numerous transcriptional factors, including activation protein-1 (AP-1) and nuclear factor-κB (NF-κB), which trigger the expression of a large number of genes encoding inflammatory mediators and cytokines [Hamilton et al., 1998]. The effects of oxLDL on the signaling pathways and the events involved in caveolin-1 expression on macrophages are poorly understood. In this study, caveolin-1 expression and the association of caveolin-1 with macrophages were evaluated in cholesterol-fed rabbits and apo-E-deficient mice. RAW264.7 macrophages were also used to test the effect of oxLDL on caveolin-1 expression and to explore the mechanisms involved. The results showed that caveolin-1 expression was increased in atherosclerotic lesions and was closely associated with macrophages in apo-E-deficient mice and cholesterol-fed rabbits. OxLDL upregulated caveolin-1 expression in RAW264.7 macrophages by activation of the MAPKs/NF-κB pathway. In addition, caveolin-1 mediated the adherence of oxLDL-treated macrophages to endothelial cells via the same pathway.

MATERIALS AND METHODS

EXPERIMENTAL ANIMALS AND IMMUNOHISTOCHEMICAL PROCEDURES

The experimental procedures and animal care and handling conformed to the local institutional guidelines for animal care of the National Taiwan University and with the "Guide for the Care and Use of Laboratory Animals" NIH publication No. 85-23, revised 1986.

The apo-E-deficient mice were purchased from Jackson Laboratory (Bar Harbor, ME). Eight were placed on a commercial mouse chow diet for 6 months, and then moved to a 0.15% cholesterol diet (Purina Mills, Inc., USA) with water available ad libitum. C57BL/6 mice fed with the normal diet were used as the controls. The mice were allowed free access to the diets for 3 months during the experiment and were bled periodically for assessment of liver and renal function. After 3 months on the diet, the animals were deprived of food overnight, then were killed by intraperitoneal injection of 35–40 mg/kg of sodium pentobarbital and the thoracic aorta gently dissected free of adherent tissue, rinsed with ice-cold phosphate-buffered saline (PBS), immersion fixed in 4% buffered paraformaldehyde, paraffin-embedded, and cross-sectioned for immunohistochemistry. To examine the expression of caveolin-1 protein and whether it was associated with macrophages, immunohistochemistry was performed on serial sections of aortas, which were deparaffinized, rehydrated, and washed with PBS. Non-specific binding was blocked by preincubation for 1 h at room temperature with PBS containing 5 mg/ml of bovine serum albumin. The first section was incubated for 1 h at 37°C with rabbit anti-human caveolin-1 antibodies (1:50 dilution; Chemicon, CA, USA) and the second section with mouse monoclonal anti-human macrophage antibody (HAM 56, 1:50; Dakocytomation, USA). The sections were then incubated for 1 h at room temperature with horseradish peroxidase (HRP)-conjugated goat anti-rabbit or anti-mouse IgG antibodies (1:100; Chemicon), followed by incubation with 0.5 mg/ml of 3,3′-diaminobenzidine/0.01% hydrogen peroxide in 0.1 M Tris–HCl buffer, pH 7.2, as chromogen (Vector Lab, USA) and observed by light microscopy. In negative controls, the primary antibodies were omitted.

Twelve male New Zealand white rabbits (2.5–3.0 kg) were fed with regular chow (control group) or regular chow enriched with 2% (w/w) cholesterol (Purina Mills, Inc.) for 6 weeks to induce hypercholesterolemia, then were killed by intravenous injection of 35–40 mg/kg of sodium pentobarbital and the aortas processed for immunohistochemical staining as described above using mouse anti-human caveolin-1 antibody (1:100; BD Transduction Laboratories, KY, USA) and mouse anti-rabbit macrophage antibody (1: 200, RamII; Dako, USA). Additional experiments were also conducted to assess the caveolin-1 expression associated with other cell types in atherosclerotic lesions, serial sections were incubated with mouse anti-human von-Willebrand factor (vWF, 1:25; Neomarkers, USA), mouse anti-human CD8 (1:1; Carpintera, USA), and mouse anti-α-smooth muscle actin (1:50, 1A4; DakoCytomation) for 1 h at 37°C, which identifies endothelial cells, T-lymphocyte, and vascular smooth muscle cells, respectively.

CULTURE OF RAW264.7 MACROPHAGES AND HUMAN UMBILICAL VEIN ENDOTHELIAL CELLS (HUVECS)

RAW264.7 murine macrophage-like cells, obtained from the American Type Culture Collection (MD, USA), were grown in DMEM containing 10% FBS and 1% antibiotic/antimyotic solution (Gibco, USA).

HUVECs isolated from human umbilical cord veins by collagenase treatment were grown in M199 medium supplemented with 20% FBS, 1% antibiotic/antimyotic solution, and 10 μg/ml of endothelial cell growth supplement at 37°C in humidified 5% CO_2/95% air and were used at passages 2–5. Cultured cells were identified as endothelial cells based on their morphology and the presence of vWF using indirect immunofluorescent microscopy.

EFFECT OF oxLDL ON CELL VIABILITY

Macrophages were plated at a density of 10^4 cells/well in 96-well plates. After overnight growth, the cells were incubated for 24 h with different concentrations of oxLDL, then cell viability was measured using the 3-(4,5-dimethylthiazol-2-yl)-2,5-diphenyl tetrazolium bromide (MTT) assay. In brief, MTT (0.5 mg/ml) was applied to the cells for 4 h to allow its conversion into formazan crystals, then, after washing with PBS, the cells were lysed with dimethyl sulfoxide and the absorbance read at 590 nm on an ELISA reader. The optical density after oxLDL treatment was used as a measure of cell viability and was normalized to that of cells incubated in control medium, which were considered 100% viable.

PREPARATION OF MEMBRANE AND CYTOSOLIC FRACTIONS AND CELL LYSATE

To prepare cell lysate, cells were lysed for 1 h at 4°C in 20 mM Tris–HCl, 150 mM NaCl, 1 mM EDTA, 1 mM EGTA, 1% Triton X-100, 1 mM PMSF, pH 7.4, then the lysate was centrifuged at 4,000*g* for 30 min at 4°C and the supernatant kept.

To prepare membrane and cytosolic proteins, cells were washed with PBS, pelleted, and dissolved in lysis buffer consisting of 1 mM EDTA, 20 mM potassium phosphate buffer, pH 7.0, 0.5 μg/ml of leupeptin, 0.7 μg/ml of pepstatin, 10 μg/ml of aprotinin, and 0.5 mM phenylmethylsulfonyl fluoride on ice, frozen three times at −80°C, and sonicated. The lysates were centrifuged at 29,000*g* at 4°C for 20 min and the resulting membrane pellet and supernatant (cytosolic fraction) stored at −80°C for Western blot analysis.

KNOCKDOWN OF GENE EXPRESSION USING INTERFERING RNA

Knockdown of ERK, p38, or JNK gene expression was performed by transfection with small interfering RNA (siRNA). Cells (5×10^6) plated on six-well plates were transfected with siRNA when they reached 30–50% confluence, according to the manufacturer's protocol. Briefly, gene-specific siRNA oligomers (200 μM) were diluted in 500 μl of Opti-MEM I reduced serum medium (Opti-MEM; Invitrogen, CA, USA) and mixed with 5 μl of each transfection reagent (Invitrogen) pre-diluted in 500 μl of Opti-MEM. After 20 min incubation at room temperature, the complexes were added to the cells in a final volume of 1 ml of medium. The ERK siRNAs (Catalog # 10620319 124945 F11 and 10620318 124945 F12; Invitrogen) were AUAUUCUGUCAGGAACCCUGUGUGA and UCACACAGGGUUCCUGACAGAAUAU, the p38 siRNAs (Catalog # 10620319 124945 F09 and 10620318 124945 F10) UUCAUUCACAGCUAGAUUACUAGGU and ACCUAGUAAUCUAGCUGUGAAUGAA, and the JNK siRNA (Catalog # 10620319 124945 G01 and10620318 124945 G02) AUCUGAAUCACUUGCAAAGAUUUG and CAAAUCUUUGCCAAGUGAUUCAGAU. Cells were transfected for 48 h. The Stealth RNAi Negative Control Med GC that has no homology to the vertebrate transcriptome was used as a negative control (siCL). The siRNA results were evaluated by Western blotting. In an additional experiment, some cells were transfected of human NF-κB p65siRNA (GAUUGAGGAGAACGUAAAtt and UUUACGUUUCUCCUCAAUCaa) or scrambled siRNA (CCUACGCCACCAAUUUCGUtt and ACGAAAUUGGUGGCGUAGGaa), while the remaining procedures of transfection are similar to that of the above method.

WESTERN BLOT ANALYSIS

Western blot analyses were performed as described previously [Chen et al., 2002]. An aliquot of sample (20 μg of total protein) was subjected to 12% SDS–PAGE electrophoresis and transferred to PVDF membranes, which were then blocked for 1 h at room temperature with 1% BSA in PBS–0.05% Tween 20. To measure caveolin-1 levels, the membranes were incubated with rabbit anti-human caveolin-1 antibodies, then with HRP-conjugated goat anti-rabbit IgG antibodies, bound antibody being detected using Chemiluminescence Reagent Plus (NEN). The intensity of each band was quantified using a densitometer. Anti-β-actin antibodies (1:10,000; Oncogen) were used to quantify β-actin, used as the internal control. In other studies, the antibodies used were rabbit anti-human phospho-JNK, mouse anti-human phopho-ERK1/2, rabbit anti-human phospho-p38, rabbit anti-human total JNK, rabbit anti-human total ERK1/2, goat anti-human total p38, and mouse anti-human NF-κB p65 (all 1:1,000; Cell Signaling), followed by HRP-conjugated goat anti-rabbit IgG antibodies (1:3,000; Sigma) or goat anti-mouse IgG or rabbit anti-goat IgG antibodies (1:3,000; Chemicon), as appropriate.

QUANTITATIVE REAL-TIME-PCR

Cellular RNA was extracted using a TRIzol reagent kit (Invitrogen). Quantitative RT-PCR was performed using a Brilliant II SYBR Green QRT-PCR master mix kit (Stratagene, CA, USA). Each reaction mix (25 μl of final volume) contained 12.5 μl of 2× SYBR QRT-PCR master mix, upstream and downstream primers (100 nM), 0.375 μl of reference dye, and 1 μl of StrataScript RT/RNase block enzyme mixture. Real-time fluorescence monitoring and melting curve analysis were performed using a Stratagene Mx3000P® real-time PCR system. The caveolin-1-specific oligonucleotide primer pair consisted of the forward primer CTACAAGCCCAACAACAAGGC and the reverse primer AGGAAGCTCTTGATGCACGGT. To quantify and prove the integrity of the isolated RNA, RT-PCR analysis for β-actin was carried out using the forward and reverse primers CTGGACTTCGAGCAAGAGATG and TGATGGAGTTGAAGGTAGTTTCG. The PCR conditions were 50°C for 60 min, 95°C for 10 min, and 40 cycles of 95°C for 30 s, 60°C for 30 s, and 68°C for 60 s for all genes assayed. Data were analyzed using Stratagene MxPro-Mx3000P QPCR software version 3.00 (Stratagene). Real-time PCR monitoring was performed with measuring the fluorescent signal at the end of the annealing phase for each cycle. Levels of caveolin-1 mRNA were normalized to β-actin mRNA levels.

LENTIVIRUS FOR DELIVERY OF shRNA

The pLKO.1-puro lentiviral vector expressing a caveolin-1 short hairpin (sh)RNA (NM001753) was purchased from Sigma. The

lentiviral packaging plasmid pCMV-dR8.91 dvpr and envelope plasmid pMD.G were obtained from the Genomic Research Center, Academia Sinica. Macrophages were co-transfected with the shRNA lentiviral plasmid, pCMV-dR8.91 dvpr, and pMD.G for the production of lentiviral particles. Transfections were carried out using jetPEI^{TM} (Polyplus transfection) and virus was harvested 72 h after transfection.

IMMUNOCYTOCHEMICAL LOCALIZATION OF NF-κB P50

To examine NF-κB expression in situ, confluent RAW264.7 macrophages on slides were exposed to oxLDL (40 μg/ml) for 30 min, then fixed in 4% paraformaldehyde in PBS for 15 min at 4°C, washed with PBS, blocked for 1 h at room temperature with 5% BSA in PBS, and incubated for 1 h at room temperature with rabbit anti-human NF-κB p50 antibodies (1:50; Neomarkers). After washes, the slides were incubated for 1 h at 37°C with fluorescein isothiocyanate (FITC)-conjugated goat anti-mouse IgG antibodies, then viewed on a fluorescent microscope.

NUCLEAR EXTRACT PREPARATION AND ELECTROPHORETIC MOBILITY SHIFT ASSAY (EMSA)

The preparation of nuclear protein extracts and the conditions for the EMSA have been described previously [Lin et al., 2004]. The 22-mer synthetic double-stranded oligonucleotides used as NF-κB probes in the gel shift assay were 5′-AGT TGA GGG GAC TTT CCC AGG C-3′ and 3′-TCA ACT CCC CTG AAA GGG TCC G-5′.

ENDOTHELIAL CELL–LEUKOCYTE ADHESION ASSAY

The cell adhesion assay was performed using a modification of previously described method [Liu et al., 2004]. The features of the assay include the non-polar fluorogenic fluorescein derivatives which in esterified form (BCECF/AM, acetoxymethyl ester BCECF/AM) readily pass through the cell membrane of viable cells; once these dyes have entered the cell, they are hydrolyzed by intracellular esterases producing polar fluorescent molecules that are retained in the cytoplasm. Macrophages were incubated for 24 h at 37°C with growth medium alone or supplemented with 40 μg/ml of oxLDL, then were labeled for 30 min at 37°C with 10 μM BCECF/AM (Boehringer-Mannheim, Mannheim, Germany) in serum-free DMEM media, washed with PBS to remove free dye, and resuspended in DMEM containing 2% FBS. HUVECs (5×10^5 cells/well) were distributed into 24-well plates and allowed to reach confluence, then labeled macrophages (10^6 cells) were added to each HUVEC-containing well and incubation continued for 15 min. Non-adherent cells were removed by two gentle washes with PBS and the degree of macrophage adhesion to HUVECs evaluated both by fluorescence microscopy and on a dual scanning spectrofluorimeter (Ex 485 nm and Em 535 nm, Spectramax Gemini XS; Molecular Devices, Sunnyvale, USA) after lysing the cells with lysis buffer.

STATISTICAL ANALYSIS

Values are expressed as the mean ± SEM. Statistical evaluation was performed using one-way ANOVA followed by the Dunnett test, with a P-value <0.05 being considered significant.

RESULTS

EXPRESSION OF CAVEOLIN-1 IN MACROPHAGES IN ATHEROSCLEROTIC LESIONS IN THE THORACIC AORTA OF CHOLESTEROL-FED RABBITS AND apo-E-DEFICIENT MICE

To examine caveolin-1 expression and the cellular localization of caveolin-1 during atherosclerosis in rabbits and mice, immunohistochemical staining with antibodies against caveolin-1, macrophages, endothelial cells, or smooth muscle cells was carried out on serial sections (Fig. 1). In the control rabbit group, caveolin-1 staining was seen in several parts of the luminal surface and a few areas of tunica adventitia (Fig. 1A). The expression of caveolin-1 in the tunica intima was associated with endothelial cells. No macrophages were present in the vascular wall and smooth muscle cells were present in the tunica media. In contrast, the aorta of cholesterol-fed rabbits showed a markedly thickened intima, which stained strongly for caveolin-1, whereas little caveolin-1 expression was detected in the underlying media. The increased caveolin-1 expression was present in macrophages, endothelial cells, smooth muscle cells, or T-lymphocytes (Fig. 1B). The distribution of caveolin-1 expression in C57BL6 control mice (Fig. 1C) was similar to that of normal rabbit. The caveolin-1 expression in apo-E-deficient mice was also similar to that in cholesterol-fed rabbits. Strong caveolin-1 staining was seen in atherosclerotic lesions and was closely associated with macrophages (Fig. 1D). Caveolin-1 expression was also present in endothelial cells or in smooth muscle cells. To determine whether caveolin-1 expression preceded the appearance of atherosclerotic lesions, we examined arterial sites without visible lesions and found a very thin intima with caveolin-1 only being detected on the luminal surface (Fig. 1E), as in control C57BL6 mice (Fig. 1B).

EXPRESSION AND TRANSLOCATION OF CAVEOLIN-1 IN oxLDL-STIMULATED MACROPHAGES

To investigate the effect of oxLDL on caveolin-1 expression at the protein level, RAW264.7 cells were incubated with oxLDL to examine the concentration dependency (0–80 μg/ml of oxLDL for 24 h) or the time dependency (12, 24, or 48 h using 40 μg/ml of oxLDL) of caveolin-1 expression by Western blotting. After 24 h incubation with 20, 40, or 80 μg/ml of oxLDL, caveolin-1 expression in the total cell lysate was, respectively, 1.6 ± 0.2-, 2.5 ± 0.3-, or 3.1 ± 0.2-fold higher than in control cells (Fig. 2A). When macrophages were incubated for 12, 24, or 48 h with 40 μg/ml of oxLDL, caveolin-1 expression was 1.4 ± 0.1-, 2.2 ± 0.3-, or 2.4 ± 0.2-fold higher, respectively, than in control cells (Fig. 2B). In contrast, incubation for 24 h with 40 μg/ml of nLDL did not affect caveolin-1 expression (Fig. 2C). Because the increase in caveolin-1 levels in response to 40 μg/ml of oxLDL was time dependent up to 24 h with no evidence of cellular damage as assessed using the MTT assay (data not shown), all subsequent Western blot experiments were performed using 40 μg/ml of oxLDL for 24 h. The effect of oxLDL was also studied by immunofluorescent staining and confocal microscopy (Fig. 2D). In untreated cells, caveolin-1 expression was weak. In contrast, cells treated for 24 h with 40 μg/ml of oxLDL showed strong caveolin-1 expression in both the cytoplasm and membrane.

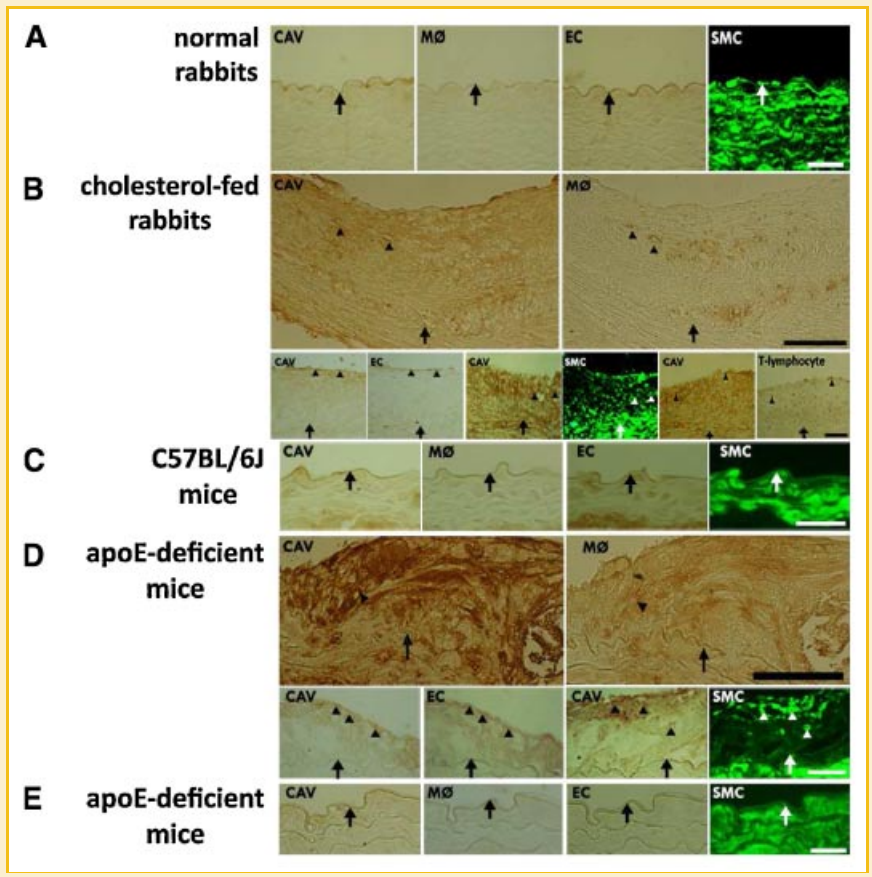

Fig. 1. The distribution of caveolin-1 (CAV) was detected in sections of thoracic aorta from normal rabbits (A), cholesterol-fed rabbits (B), C57BL6 control mice (C), and apo-E-deficient mice (D,E) by immunohistochemistry. The weak caveolin-1 staining is seen at the luminal surface of normal animals and was present in endothelial cells (EC) (A,C). No macrophages (Mϕ) were present in the vascular wall and smooth muscle cells (SMC) were present on the tunica media. Strong caveolin-1 staining (arrowheads) is seen in the markedly thickened intima of cholesterol-fed rabbits and is closely co-localized with macrophages, endothelial cells, smooth muscle cells, and T-lymphocyte, respectively (B). The expression of caveolin-1 is also present in macrophages, endothelial cells, or smooth muscle cells in atherosclerotic lesions of apo-E-deficient mice (D), while normal regions in apo-E-deficient mice showed only caveolin-1 expression was in the luminal surface (E). The lumen is uppermost in all sections. The internal elastic membrane is indicated by an arrow. Bar = 100 μm. [Color figure can be viewed in the online issue, which is available at www.interscience.wiley.com.]

To determine whether the changes in caveolin-1 protein levels were associated with changes in mRNA levels, quantitative real-time PCR was performed. The results (Fig. 2E) showed that non-stimulated macrophages produced low amounts of caveolin-1 mRNA and that 4 h treatment with 40 μg/ml of oxLDL resulted in a marked increase in levels, whereas nLDL treatment had no effect. Furthermore, the addition of 20 μg/ml of actinomycin D (an RNA polymerase inhibitor) or cycloheximide (a protein synthesis inhibitor) for 1 h before incubation with oxLDL for 4 h significantly reduced caveolin-1 mRNA expression, showing that oxLDL-induced caveolin-1 expression requires de novo RNA and protein synthesis.

We then determined whether this effect of oxLDL was associated with translocation of caveolin-1 in macrophages, as this translocation mechanism has been reported to play an important role in atherosclerosis [Fielding and Fielding, 2001]. Macrophages were treated with 40 μg/ml of oxLDL for 24 h, then cytosolic and plasma membrane fractions were prepared and immunoblotted for caveolin-1. As shown in Figure 3A (cytoplasmic fraction) and B (membrane fraction), caveolin-1 translocation to the membrane and an increase in the caveolin-1 content of both the cytosolic and membrane fractions were seen, suggesting an effect on both expression and translocation. Cells with the co-incubation of oxLDL and nLDL did not affect oxLDL-induced caveolin-1 expression.

OxLDL-UPREGULATED CAVEOLIN-1 EXPRESSION IN MACROPHAGES IS DEPENDENT ON MAPK PHOSPHORYLATION

Previous studies have shown that oxLDL can activate MAPKs in the signaling pathways leading to cytokine production [Incardona and Eaton, 2000]. In the next set of experiments, we examined whether the effects of oxLDL on caveolin-1 expression in macrophages were mediated via the ERK1/2, p38, or JNK–MAPK pathway. As shown in Figure 4A–C, phosphorylation of ERK1/2, p38, and JNK was significantly increased 15 min after addition of 40 μg/ml of oxLDL, while nLDL had no effect. The increase in caveolin-1 expression in response to oxLDL treatment was inhibited by 1 h pretreatment with

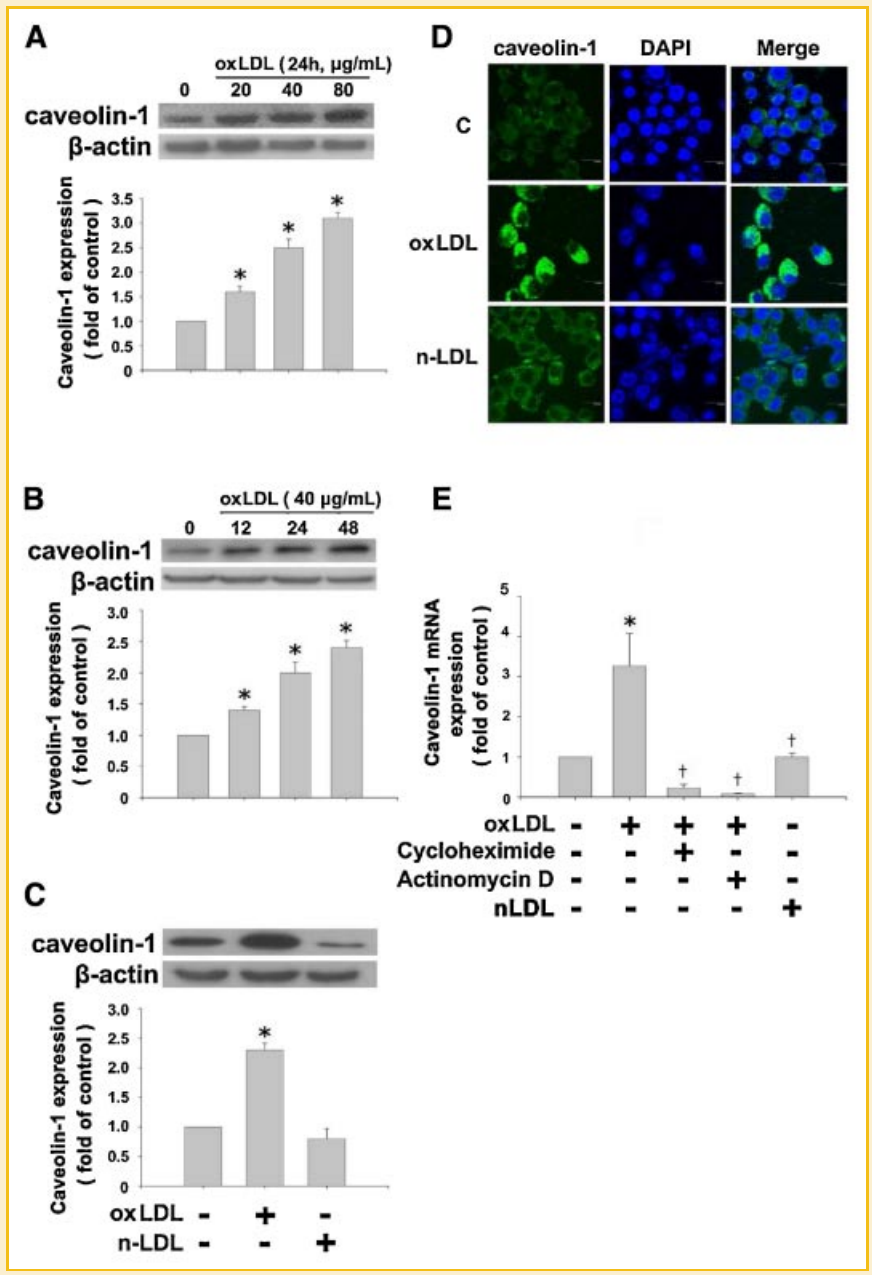

Fig. 2. OxLDL upregulates caveolin-1 mRNA and protein levels. RAW264.7 cells were incubated with 0–80 μg/ml of oxLDL for 24 h (A), with 40 μg/ml of oxLDL for 12, 24, or 48 h (B), or with 40 μg/ml of oxLDL or nLDL for 24 h (C), then caveolin-1 expression in whole cell lysates was measured by Western blotting. β-actin was used as the loading control. D: The cells were treated as in (C), then the distribution of caveolin-1 was analyzed by immunofluorescent staining and confocal microscopy. Caveolin-1 expression is indicated by green fluorescence (FITC) and nuclei by blue fluorescence (DAPI). Bar = 20 μm. E: Analysis of caveolin-1 mRNA levels in untreated macrophages or macrophages preincubated for 1 h with cycloheximide (20 μg/ml) or actinomycin D (20 μg/ml), then for 4 h with 40 μg/ml of oxLDL. Total RNA was analyzed by quantitative real-time PCR after normalization to β-actin mRNA. In A–C and E, the data are expressed as a fold level of the control value and are the mean ± SEM for five separate experiments. $^{*}P < 0.05$ compared to untreated cells. $^{\dagger}P < 0.05$ compared to oxLDL-treated cells. [Color figure can be viewed in the online issue, which is available at www.interscience.wiley.com.]

30 μM PD98059 (an ERK1/2 inhibitor), SB203580 (a p38 inhibitor), or SP600125 (a JNK inhibitor) (Fig. 4D) and also by transfection of macrophages with ERK1/2, p38, or JNK-specific siRNA (100 μmol/ml) (Fig. 4E). The effectiveness of the siRNA treatment was validated by results showing that p38-, ERK1/2-, or JNK-specific siRNA (compared to control siRNA) caused a 85-, 55-, or 75% reduction in p38, ERK1/2, or JNK protein expression, respectively (Fig. 4F).

OxLDL INCREASES CAVEOLIN-1 EXPRESSION IN MACROPHAGES BY ACTIVATION OF NF-κB AND NUCLEAR TRANSLOCATION OF NF-κB p50

The activation of NF-κB is the key factor regulating the induction of many inflammatory cytokines [Barnes and Karin, 1997]. Gel-shift assays were performed to determine the effect of oxLDL on NF-κB activation in macrophages. As shown in Figure 5A, low basal

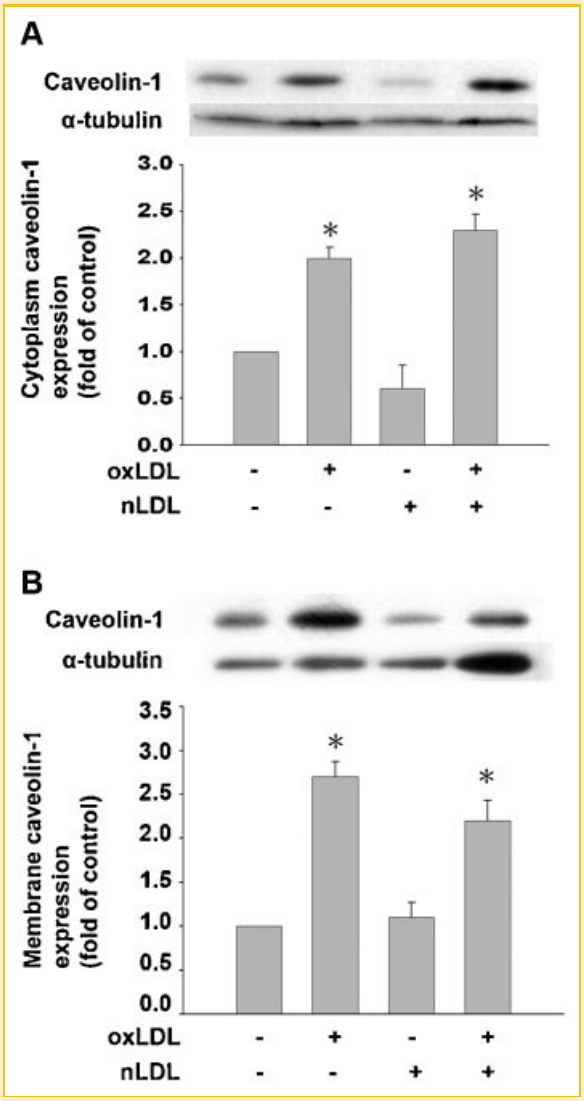

Fig. 3. OxLDL increases caveolin-1 expression and translocation from the cytosol to the membrane. Caveolin-1 levels in the cytosolic (A) and plasma membrane (B) fractions of RAW264.7 cells treated with 40 μg/ml of oxLDL or nLDL or the combination of oxLDL and nLDL for 24 h. The data are expressed as a fold level of the control value and are the mean ± SEM for three separate experiments. $^{*}P < 0.05$ compared to untreated cells.

levels of NF-κB binding activity were detected in control cells, and binding was significantly increased by 30 min treatment with 40 μg/ml of oxLDL. The binding activity was blocked by a 100-fold excess of unlabeled NF-κB probe (data not shown). The oxLDL-induced increase in NF-κB-binding activity was markedly reduced by 1 h pretreatment with 30 μM PD98059, SB203580, or SP600125. In addition, the relationship between caveolin expression and NF-κB activity was elucidated. As shown by Western blots (Fig. 5B), the oxLDL-induced increase in caveolin-1 levels was not seen when cells were incubated with a mixture of oxLDL and parthenolide, a NF-κB inhibitor [Sohn et al., 2005]. Immunochemical studies showed marked NF-κB p50 staining in the nuclei of oxLDL-treated macrophages, while control cells showed weaker nuclear NF-κB expression, but stronger staining in the cytoplasm (Fig. 5C).

Similar results were obtained with NF-κB reduction by the knockdown of p65, a subunit of NF-κB. We transfected macrophages with siRNA specific to p65. At 48 h after siRNA transfection, macrophages were immunoblotted with anti-p65 Ab. p65 expression was markedly reduced in p65-siRNA-transfected cells, whereas the control siRNA had no effect (Fig. 5D). OxLDL-induced caveolin-1 protein expression was also prevented in p65-siRNA transfected cells compared with oxLDL-treated cells alone (Fig. 5E), indicating that p65 signaling plays an important role in the mechanism of oxLDL-induced caveolin-1 expression in macrophages.

OxLDL INCREASES MACROPHAGE ADHESION TO HUVECs VIA CAVEOLIN-1

To explore whether the change in caveolin-1 expression directly impacted on vascular function and resulted in the development of atheroma, we examined whether the adhesion of oxLDL-treated macrophages to HUVECs was mediated by caveolin-1. As shown in Figure 6A, control confluent HUVECs showed minimal binding of macrophages, but adhesion was substantially increased when the macrophages were treated for 24 h with 40 μg/ml of oxLDL. The involvement of caveolin-1 in the adhesion of oxLDL-treated macrophages to HUVECs was examined by pretreatment of the cells with anti-caveolin-1 antibody or by transfection with caveolin-1-specific shRNA (100 μM). After macrophages were pretreated with 10 μg/ml of anti-caveolin-1 antibody (“cav” in the figure) or transfected with caveolin-1-specific shRNA (shRNAcav) for 24 h, then incubated with oxLDL, the binding of macrophages to HUVECs was significantly lower than in control oxLDL-treated cells, showing that caveolin-1 plays a major role in the adhesion of oxLDL-treated macrophages to HUVECs. The adherence of oxLDL-treated macrophages to HUVECs was also inhibited by 30 μM PD98059 (PD), SP600125 (SP), SB203580 (SB), or parthenolide (Pl).

DISCUSSION

The present study showed that caveolin-1 was strongly expressed in atherosclerotic lesions of cholesterol-fed rabbits and apo-E-deficient mice and was closely co-localized with macrophages. In RAW264.7 macrophages, caveolin-1 expression was increased and translocated from the cytoplasm to the cell membrane on oxLDL stimulation. This increase in caveolin-1 levels was mediated by activation of MAPK phosphorylation and NF-κB. The adherence of oxLDL-treated macrophages to endothelial cells was dependent on the increased caveolin-1 expression and this effect was also mediated through the MAPK/NF-κB pathway.

During the development of atherosclerosis, macrophages play a pivotal role in the formation of atherosclerotic lesions. These cells take up large amounts of lipids and accumulate in the subendothelial space, forming foam cells that fill the lesion area. Since caveolins have a proatherogenic role by promoting the transcytosis of LDL particles from the blood to the subendothelial space [Fielding and Fielding, 1996], it was of interest to examine the distribution of caveolins in atherosclerotic lesions and the associated cells.

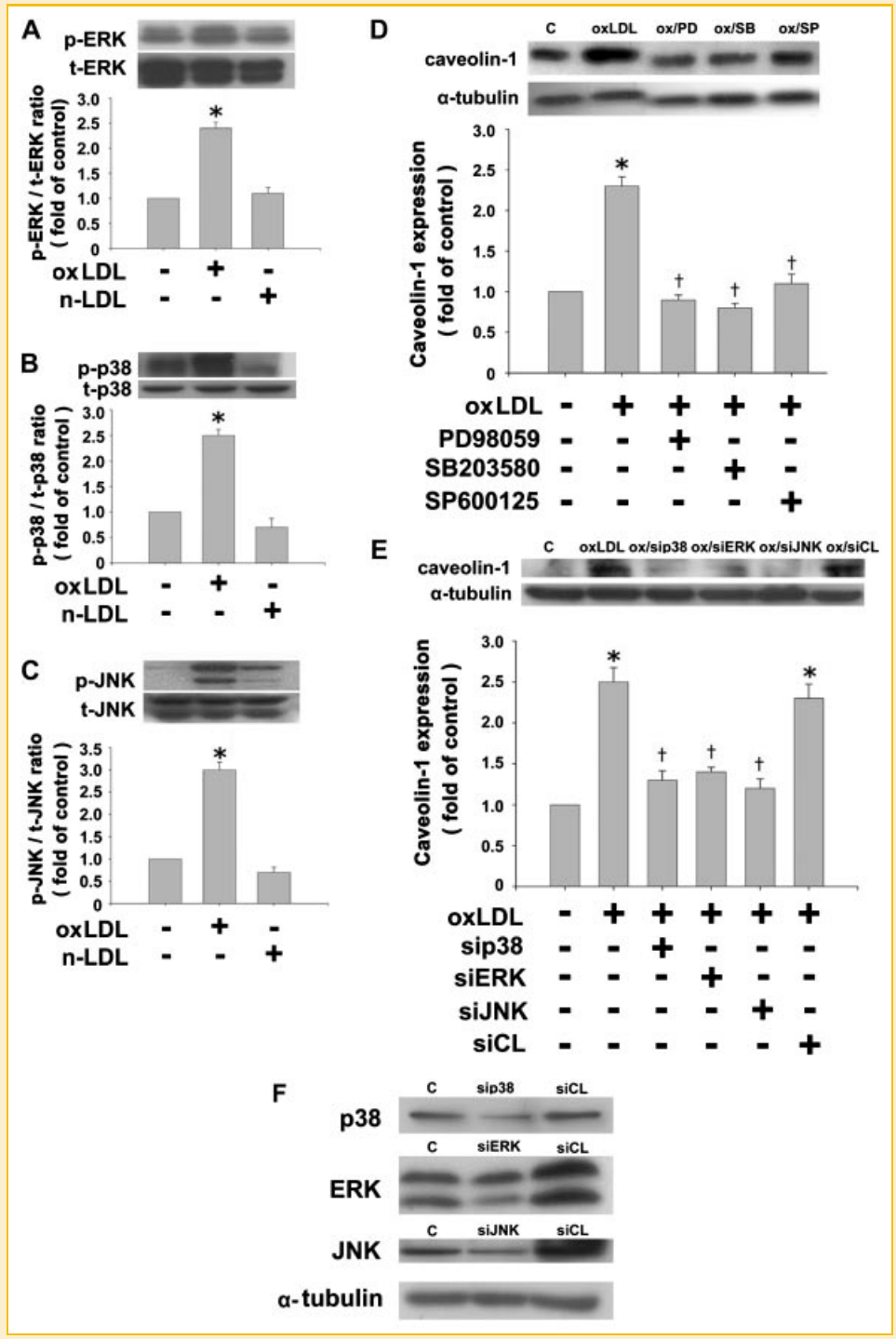

Fig. 4. OxLDL-upregulated caveolin-1 expression in RAW264.7 macrophages is dependent on phosphorylation of ERK, p38, and JNK MAPKs. A–C: Western blot analysis showing the effect of oxLDL on the phosphorylation of (A) ERK1/2, (B) p38, or (C) JNK in RAW264.7 macrophages. Macrophages were incubated with or without 40 μg/ml of oxLDL or nLDL for 15 min, then aliquots of cell lysate containing equal amounts of protein were subjected to immunoblotting with the indicated antibodies. D: Effect of inhibitors of MAPK phosphorylation on caveolin-1 expression in oxLDL-treated macrophages. Cells were incubated for 1 h with medium or 30 μM PD98059 (an ERK1/2 inhibitor), SB203580 (a p38 inhibitor), or SP600125 (a JNK inhibitor), then for 24 h with 40 μg/ml of oxLDL in the continued presence of the inhibitor, then caveolin-1 expression was measured by Western blotting. E: The oxLDL-induced increase in caveolin-1 expression is inhibited by transfection of macrophages with p38-, ERK1/2-, or JNK-specific siRNA (100 μmol/ml). F: p38-, ERK1/2-, or JNK-specific siRNA (compared to control siRNA) causes a 85%, 55%, or 75% reduction in p38, ERK1/2, or JNK protein expression. In A–E, the data are expressed as a fold value of the control. A representative result from three separate experiments is shown and the summarized data for the three experiments are shown in the bar chart. Total ERK (t-ERK), total p38 (t-p38), total JNK (t-JNK), or α-tubulin was used as the loading control for Figure 4A–C, or D and E, respectively. $^{*}P < 0.05$ compared to untreated cells. $^{\dagger}P < 0.05$ compared to oxLDL-treated cells.

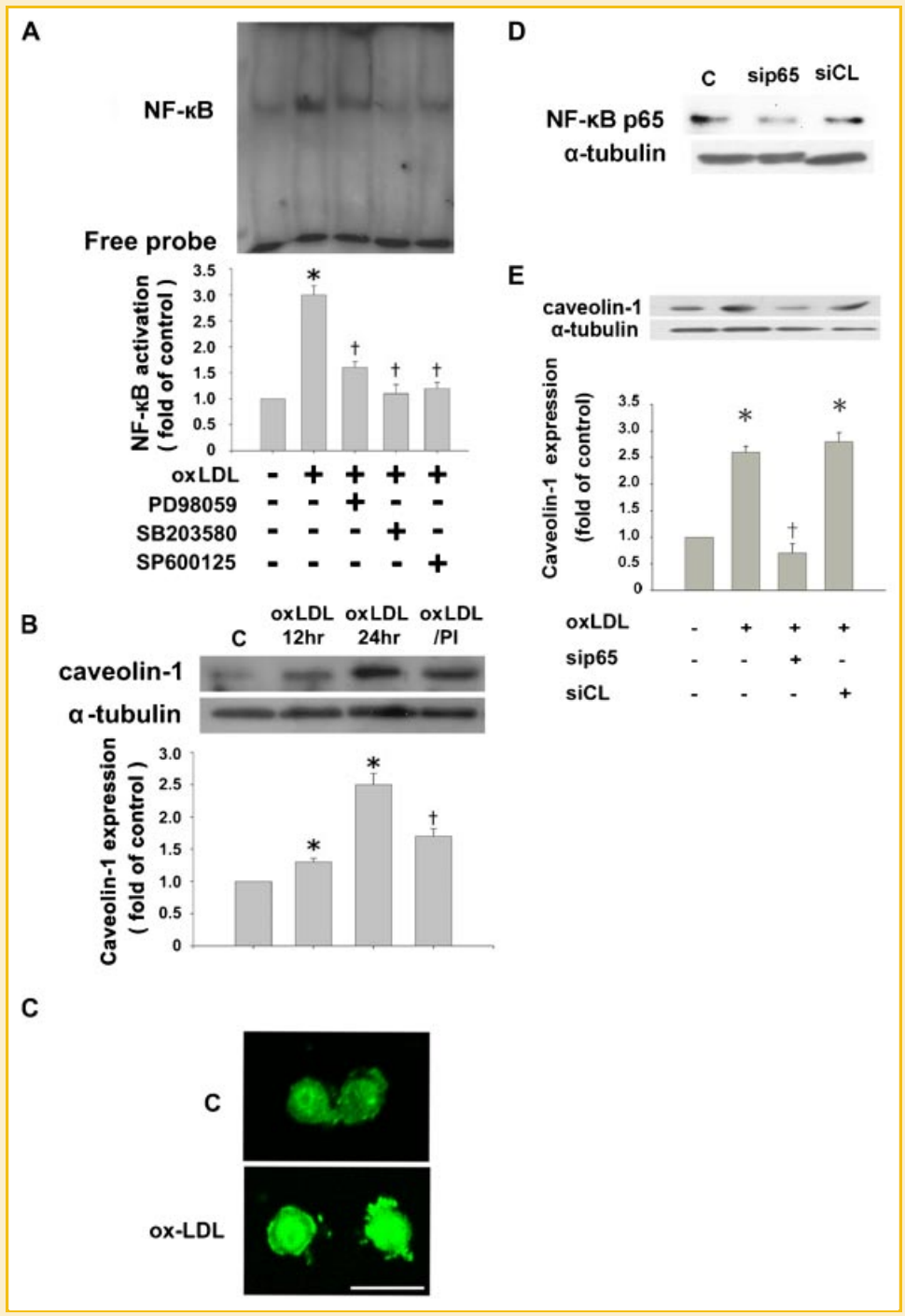

Fig. 5. OxLDL-induced upregulation of caveolin-1 expression in RAW264.7 macrophages is mediated by NF-κB activation and NF-κB p50 nuclear translocation. A: Nuclear extracts prepared from untreated cells or from cells treated for 1 h with 30 μM PD98059 (an ERK1/2 inhibitor), SB203580 (a p38 inhibitor), or SP600125 (a JNK inhibitor), then incubated with or without 40 μg/ml of oxLDL in the continued presence of the inhibitor for 30 min were tested for NF-κB DNA binding activity by EMSA. B: Cells were incubated for 12 or 24 h with 40 μg/ml of oxLDL or for 24 h with 40 μg/ml of oxLDL and 30 μM parthenolide (PI), an NF-κB inhibitor, then cell lysates were prepared and assayed for caveolin-1 on Western blots. In A,B, a representative result from three separate experiments is shown and the summarized data for the three experiments are shown in the bar chart. C: Immunofluorescent staining for NF-κB p50. Higher expression of NF-κB p50 protein is seen in the nuclei of oxLDL-stimulated macrophages compared to control cells. Bar = 20 μm. D: NF-κB p65-specific siRNA reduced NF-κB p65 protein expression compared with non-treated cells (C) and control siRNA-transfected cells (siCL). At 48 h after transfection, cells were lysed and immunoblotted with anti-p65 Ab. The membrane was stripped and probed with anti-α-tubulin Ab for loading control. The experiment was repeated three times with similar results. E: p65 knockdown prevents oxLDL-induced caveolin-1 expression. At 48 h after transfection, cells were exposed to oxLDL (40 μg/ml) for 24 h. After oxLDL stimulation, cells were lysed and immunoblotted with anti-caveolin-1 Ab. The membrane was stripped and probed with anti-α-tubulin Ab for loading control. $^{*}P < 0.05$ compared to untreated cells, $^{\dagger}P < 0.05$ compared to oxLDL-treated cells. [Color figure can be viewed in the online issue, which is available at www.interscience.wiley.com.]

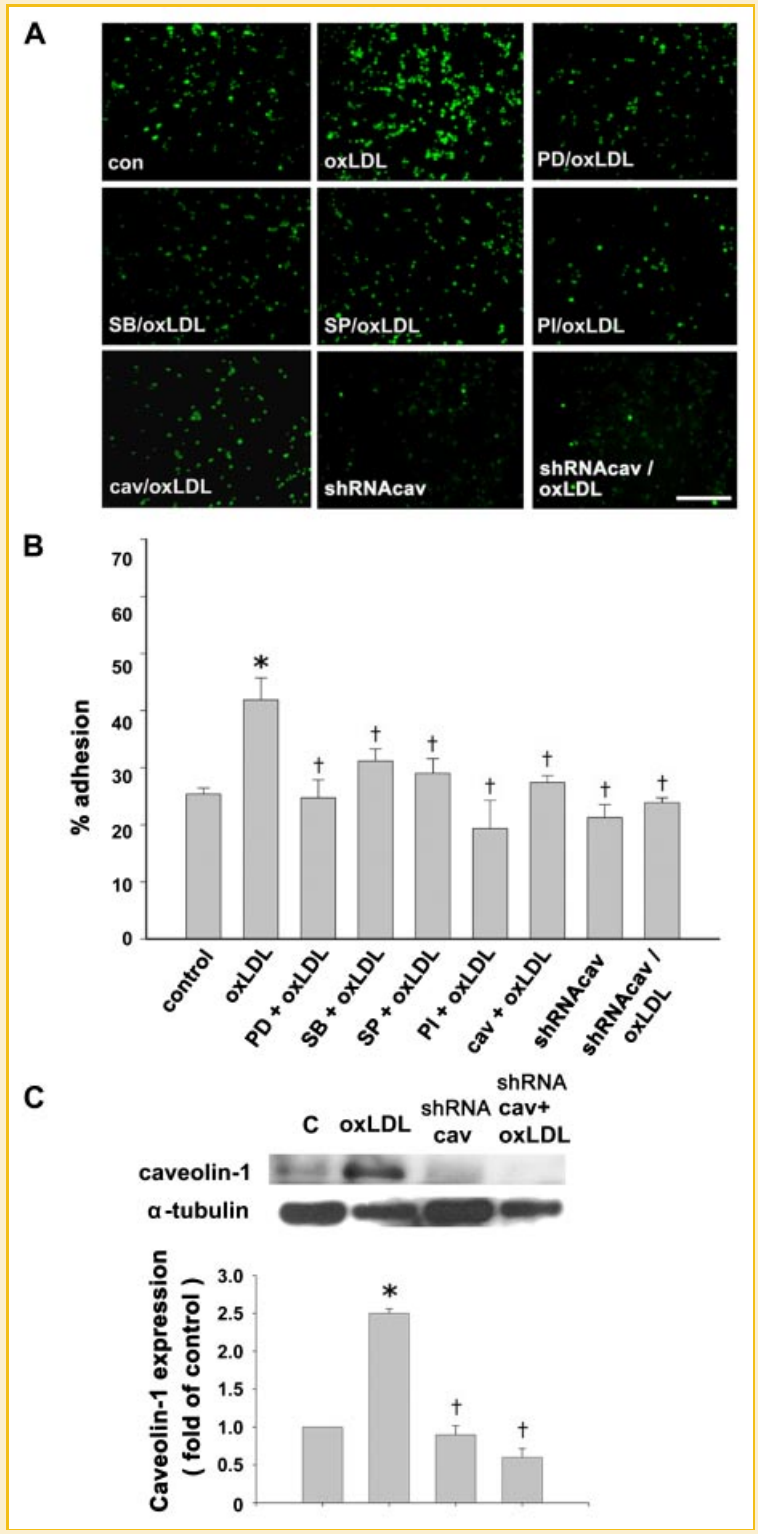

Fig. 6. OxLDL increases macrophage adhesion to HUVECs via caveolin-1. A,B: Cells were left untreated or were pretreated for 24 h with 30 μM PD98059 (PD), SB203580 (SB), SP600125 (SP), or parthenolide (PI), 10 μg/ml of anti-caveolin-1antibody (cav), or 100 μM caveolin-1-specific shRNA (shRNAcav), then with 40 μg/ml of oxLDL for 24 h in the continued presence of the inhibitor. A: Representative fluorescent photomicrographs showing the effect on macrophage adhesion to HUVECs. Con is untreated cells. Bar = 100 μm. B: Macrophage adherence shown as % adhesion. C: Transfection of macrophages with caveolin-1 shRNA (100 μM) causes a significant reduction in the oxLDL-induced increase in caveolin-1 expression. The data are the mean ± SEM for five separate experiments. $^{*}P < 0.05$ compared to untreated cells. $^{\dagger}P < 0.05$ compared to oxLDL-treated cells.

Caveolin-1 immunoreactivity is increased in the diseased radial artery in both rabbits and humans [Zulli et al., 2006] and caveolin-1 expression is high in the arterial intima after 5 weeks of a high cholesterol diet in hypercholesterolemic rabbits [Lin et al., 2006]. The loss of caveolin-1 gene expression in caveolin-1/apo-E double-knockout mice is clearly protective against the development of aortic atheromas, with up to 70% reduction in atherosclerotic lesion area compared to the single apo-E knockout controls [Frank et al., 2004]. In the present study, we demonstrated that caveolin-1 was strongly expressed in atherosclerotic lesions of the thoracic aorta in cholesterol-fed rabbits and apo-E-deficient mice compared to the adjacent normal vascular area and control animals. Caveolin-1 expression was closely associated with macrophages. Taken together, these results suggest that caveolin-1 is closely associated with blood vessel disease and may be a novel target for drug development in the pharmacologic prevention of atheroma formation.

Evidence for caveolin-1 expression by macrophages in in vitro studies is scarce and conflicting [Gargalovic and Dory, 2003]. Fielding and Fielding [1997] reported that macrophages do not express caveolin protein. In contrast, immunofluorescence labeling suggested that caveolin-1 protein is expressed in mouse bone marrow-derived macrophages [Baorto et al., 1997]. Immunoblot analyses also indicated caveolin-1 expression in THP-1 cells, but not in J774 or RAW264.7 macrophages, while none of these cells expressed caveolin-2 [Matveev et al., 1999]. In contrast, caveolin-1 mRNA was recently detected in J774 and RAW264.7 macrophages by RT-PCR [Lei and Morrison, 2000; Gargalovic and Dory, 2001]. In the present study, we demonstrated that significant caveolin-1 expression was induced in RAW264.7 macrophages on oxLDL stimulation using the three independent approaches of real-time PCR, Western blotting, and immunofluorescent staining. In addition, oxLDL also resulted in an increase in the caveolin-1 content of both the cytosolic and membrane fractions compared to control cells, suggesting an effect on both expression and translocation. Furthermore, to test whether transcriptional regulation was involved in the induction of caveolin-1 by oxLDL, actinomycin D and cycloheximide were used to prevent the transcription of new mRNA and inhibit the synthesis of cytoplasmic protein, respectively, and either reagent blocked oxLDL-induced caveolin-1 mRNA upregulation. These results indicate that both transcriptional and posttranscriptional mechanisms are involved in the regulation of caveolin-1 expression.

In many cell types, including macrophages, oxLDL activates signal transduction cascades, thus affecting foam cell formation [Berliner and Heinecke, 1996]. Signal transduction pathways, including the MAPK pathway, play a crucial role in the regulation of caveolin-1 protein expression and membrane trafficking [Incardona and Eaton, 2000]. Our study showed that oxLDL caused strong activation of three MAPK members in macrophages. SB203580, a specific p38 inhibitor, prevents oxLDL-exposed J774 cells from becoming foam cells [Zhao et al., 2002] and oxLDL induces macrophage proliferation by ERK and JNK activation [Senokuchi et al., 2004] and modulates PPARγ activity through JNK MAPK phosphorylation in human THP-1 macrophages [Yin et al., 2006]. Oxidative stress (H_2O_2) induces p38-mediated upregulation of caveolin-1 in normal human mammary epithelial cells [Dasari et al., 2006]. Regional myocardial ischemia-induced activation of ERK is associated with subcellular redistribution of caveolin-1 [Ballard-Croft et al., 2006]. In contrast, caveolin-1 null mice develop cardiac hypertrophy, with hyperactivation of ERK in cardiac fibroblasts [Cohen et al., 2003]. In the present study, the increase in caveolin-1 expression induced by oxLDL was markedly suppressed in the presence of an ERK inhibitor (PD98059), a p38 inhibitor (SB203580), or a JNK inhibitor (SP600125), as well as by MAPK-specific siRNA. The different involvement of MAPK activation seen in these studies may be related to differences in cell types and the induced function. To our knowledge, our study is the first to show that caveolin-1 expression in oxLDL-treated macrophages is mediated through the phosphorylation of three different MAPK members.

Recent data indicate that enhanced plasma oxLDL levels increase NF-κB activation in the blood of patients with unstable angina and that the increase is mainly due to the activation of monocytes [Cominacini et al., 2005]. It is now documented that exposure of cells to minimally oxLDL and specific oxidized phospholipids leads to upregulation of adhesion molecules, proinflammatory cytokines, and growth factors and to vascular dysfunction [Napoli et al., 2001]. We have previously demonstrated that the leukocyte–endothelial interaction was enhanced in cholesterol-fed rats [Lu et al., 2007]. In the present study, oxLDL treatment caused an increase in NF-κB-binding activity and translocation. We also demonstrated that oxLDL increased caveolin-1 expression via the increase in NF-κB activity and that NF-κB transcriptional activity was modulated by phosphorylation by MAPKs.

Atherosclerotic lesions result from the adherence of monocytes/macrophages to endothelial cells and their accumulation within the arterial intima [Boyle, 2005]. Given the probable involvement of caveolin-1 in leukocyte recruitment to early atherosclerotic lesions, our findings suggest an additional mechanism by which caveolin-1 expression in macrophages may be involved in the progression of atherosclerosis. In the present study, anti-caveolin-1 antibodies inhibited the adhesion of oxLDL-treated macrophages to endothelial cells. We also showed that a decrease in endogenous caveolin-1 levels in macrophages by siRNA treatment reduced the binding of oxLDL-treated macrophages to endothelial cells. These results demonstrate, for the first time, that oxLDL-induced caveolin-1 production is involved in macrophage adhesion to endothelial cells. This concept is consistent with the view that caveolin-1 expression can be upregulated, and that, once expressed, caveolin-1 can greatly enhance cancer cell adhesion and stimulate de novo focal adhesion in protrusive cellular regions [Bailey and Liu, 2008; Goetz et al., 2008]. Gastric tumor cell adhesion to the endothelium is mediated by the co-localization of caveolin-1 and vascular cell adhesion molecule-1 [Shin et al., 2006]. The oxLDL-induced increase in monocyte–endothelial cell adhesion, acting via caveolin-1 expression, has important implications in terms of atherogenic mechanisms, as well as in the treatment of atherosclerosis.

In conclusion, in this study, we demonstrate that caveolin-1 expression is increased in macrophages in atherosclerotic lesions of cholesterol-fed rabbits and apo-E-deficient mice. Caveolin-1 expression in mouse macrophages is significantly upregulated in vitro by oxLDL and this effect is mediated by MAPK

phosphorylation and NF-κB activation. In addition, oxLDL increases the adhesion of macrophages to endothelial cells via caveolin-1 expression and this adhesion is effectively reduced by anti-caveolin-1 antibody or caveolin-1-specific shRNA. These findings indicate the important function of caveolin-1 in enhancing macrophage adherence to endothelial cells on oxLDL stimulation, resulting in initiation of atherosclerosis.

ACKNOWLEDGMENTS

We thank Mr. Hsuan-Hao Chen and Miss Hsiang-Han Wang for technical assistance in manuscript preparation. This work was supported in part by grants from the National Science Council (NSC 96-2628-B-002-051-MY3, NSC 96-2314-B-002-150-MY3, NSC 95-2752-B-006-005-PAE, and NSC 95-2314-B-002-123), Taiwan, Republic of China.

REFERENCES

Bailey KM, Liu J. 2008. Caveolin-1 up-regulation during epithelial to mesenchymal transition is mediated by focal adhesion kinase. J Biol Chem 283:13714–13724.

Ballard-Croft C, Locklar AC, Kristo G, Lasley RD. 2006. Regional myocardial ischemia-induced activation of MAPKs is associated with subcellular redistribution of caveolin and cholesterol. Am J Physiol Heart Circ Physiol 291:H658–H667.

Baorto DM, Gao Z, Malaviya R, Dustin ML, van der Merwe A, Lublin DM, Abraham SN. 1997. Survival of FimH-expressing enterobacteria in macrophages relies on glycolipid traffic. Nature 389:636–639.

Barnes PJ, Karin M. 1997. Nuclear factor-kappaB: A pivotal transcription factor in chronic inflammatory diseases. N Engl J Med 336:1066–1071.

Berliner JA, Heinecke JW. 1996. The role of oxidized lipoproteins in atherogenesis. Free Radic Biol Med 20:707–727.

Boyle JJ. 2005. Macrophage activation in atherosclerosis: Pathogenesis and pharmacology of plaque rupture. Curr Vasc Pharmacol 3:63–68.

Brown MS, Goldstein JL. 1983. Lipoprotein metabolism in the macrophage: Implications for cholesterol deposition in atherosclerosis. Annu Rev Biochem 52:223–261.

Chen YH, Lin SJ, Chen JW, Ku HH, Chen YL. 2002. Magnolol attenuates VCAM-1 expression in vitro in TNF-alpha-treated human aortic endothelial cells and in vivo in the aorta of cholesterol-fed rabbits. Br J Pharmacol 135:37–47.

Cohen AW, Park DS, Woodman SE, Williams TM, Chandra M, Shirani J, Pereira de Souza A, Kitsis RN, Russell RG, Weiss LM, Tang B, Jelicks LA, Factor SM, Shtutin V, Tanowitz HB, Lisanti MP. 2003. Caveolin-1 null mice develop cardiac hypertrophy with hyperactivation of p42/44 MAP kinase in cardiac fibroblasts. Am J Physiol Cell Physiol 284:C457–C474.

Cohen AW, Hnasko R, Schubert W, Lisanti MP. 2004. Role of caveolae and caveolins in health and disease. Physiol Rev 84:1341–1379.

Cominacini L, Anselmi M, Garbin U, Fratta Pasini A, Stranieri C, Fusaro M, Nava C, Agostoni P, Keta D, Zardini P, Sawamura T, Lo Cascio V. 2005. Enhanced plasma levels of oxidized low-density lipoprotein increase circulating nuclear factor-kappa B activation in patients with unstable angina. J Am Coll Cardiol 46:799–806.

Dasari A, Bartholomew JN, Volonte D, Galbiati F. 2006. Oxidative stress induces premature senescence by stimulating caveolin-1 gene transcription through p38 mitogen-activated protein kinase/Sp1-mediated activation of two GC-rich promoter elements. Cancer Res 66:10805–10814.

Fielding PE, Fielding CJ. 1996. Intracellular transport of low density lipoprotein derived free cholesterol begins at clathrin-coated pits and terminates at cell surface caveolae. Biochemistry 35:14932–14938.

Fielding CJ, Fielding PE. 1997. Intracellular cholesterol transport. J Lipid Res 38:1503–1521.

Fielding CJ, Fielding PE. 2001. Caveolae and intracellular trafficking of cholesterol. Adv Drug Deliv Rev 49:251–264.

Frank PG, Woodman SE, Park DS, Lisanti MP. 2003. Caveolin, caveolae, and endothelial cell function. Arterioscler Thromb Vasc Biol 23:1161–1168.

Frank PG, Lee H, Park DS, Tandon NN, Scherer PE, Lisanti MP. 2004. Genetic ablation of caveolin-1 confers protection against atherosclerosis. Arterioscler Thromb Vasc Biol 24:98–105.

Gargalovic P, Dory L. 2001. Caveolin-1 and caveolin-2 expression in mouse macrophages. High density lipoprotein 3-stimulated secretion and a lack of significant subcellular co-localization. J Biol Chem 276:26164–26170.

Gargalovic P, Dory L. 2003. Caveolins and macrophage lipid metabolism. J Lipid Res 44:11–21.

Goetz JG, Joshi B, Lajoie P, Strugnell SS, Scudamore T, Kojic LD, Nabi IR. 2008. Concerted regulation of focal adhesion dynamics by galectin-3 and tyrosine-phosphorylated caveolin-1. J Cell Biol 180:1261–1275.

Hamilton TA, Major JA, Armstrong D, Tebo JM. 1998. Oxidized LDL modulates activation of NFkappaB in mononuclear phagocytes by altering the degradation if IkappaBs. J Leukoc Biol 64:667–674.

Incardona JP, Eaton S. 2000. Cholesterol in signal transduction. Curr Opin Cell Biol l12:193–203.

Kim MJ, Dawes J, Jessup W. 1994. Transendothelial transport of modified low-density lipoproteins. Atherosclerosis 108:5–17.

Kunsch C, Medford RM. 1999. Oxidative stress as a regulator of gene expression in the vasculature. Circ Res 85:753–766.

Lei MG, Morrison DC. 2000. Differential expression of caveolin-1 in lipopolysaccharide-activated murine macrophages. Infect Immun 68:5084–5089.

Lin SJ, Shyue SK, Liu PL, Chen YH, Ku HH, Chen JW, Tam KB, Chen YL. 2004. Adenovirus-mediated overexpression of catalase attenuates oxLDL-induced apoptosis in human aortic endothelial cells via AP-1 and C-Jun N-terminal kinase/extracellular signal-regulated kinase mitogen-activated protein kinase pathways. J Mol Cell Cardiol 36:129–139.

Lin WW, Lin YC, Chang TY, Tsai SH, Ho HC, Chen YT, Yang VC. 2006. Caveolin-1 expression is associated with plaque formation in hypercholesterolemic rabbits. J Histochem Cytochem 54:897–904.

Lisanti MP, Scherer PE, Vidugiriene J, Tang Z, Hermanowski-Vosatka A, Tu YH, Cook RF, Sargiacomo M. 1994. Characterization of caveolin-rich membrane domains isolated from an endothelial-rich source: Implications for human disease. J Cell Biol 126:111–126.

Liu J, Chow VT, Jois SD. 2004. A novel, rapid and sensitive heterotypic cell adhesion assay for CD2–CD58 interaction, and its application for testing inhibitory peptides. J Immunol Methods 291:39–49.

Lu LS, Hung LM, Liao CH, Wu CC, Su MJ. 2007. Effects of rosiglitazone on native low-density-lipoprotein-induced respiratory burst in circulating monocytes and on the leukocyte-endothelial interaction in cholesterol-fed rats. Naunyn Schmiedebergs Arch Pharmacol 375:251–260.

Matveev S, van der Westhuyzen DR, Smart EJ. 1999. Co-expression of scavenger receptor-BI and caveolin-1 is associated with enhanced selective cholesteryl ester uptake in THP-1 macrophages. J Lipid Res 40:1647–1654.

Napoli C, de Nigris F, Palinski W. 2001. Multiple role of reactive oxygen species in the arterial wall. J Cell Biochem 82:674–682.

Ross R. 1993. The pathogenesis of atherosclerosis: A perspective for the 1990s. Nature 362:801–809.

Scherer PE, Lewis RY, Volonte D, Engelman JA, Galbiati F, Couet J, Kohtz DS, van Donselaar E, Peters P, Lisanti MP. 1997. Cell-type and tissue-specific expression of caveolin-2. Caveolins 1 and 2 co-localize and form a stable hetero-oligomeric complex in vivo. J Biol Chem 272:29337–29346.

Schroeder F, Gallegos AM, Atshaves BP, Storey SM, McIntosh AL, Petrescu AD, Huang H, Starodub O, Chao H, Yang H, Frolov A, Kier AB. 2001. Recent advances in membrane microdomains: Rafts, caveolae, and intracellular cholesterol trafficking. Exp Biol Med (Maywood) 226:873–890.

Senokuchi T, Matsumura T, Sakai M, Matsuo T, Yano M, Kiritoshi S, Sonoda K, Kukidome D, Nishikawa T, Araki E. 2004. Extracellular signal-regulated kinase and p38 mitogen-activated protein kinase mediate macrophage proliferation induced by oxidized low-density lipoprotein. Atherosclerosis 176:233–245.

Shin J, Kim J, Ryu B, Chi SG, Park H. 2006. Caveolin-1 is associated with VCAM-1 dependent adhesion of gastric cancer cells to endothelial cells. Cell Physiol Biochem 17:211–220.

Sohn RH, Deming CB, Johns DC, Champion HC, Bian C, Gardner K, Rade JJ. 2005. Regulation of endothelial thrombomodulin expression by inflammatory cytokines is mediated by activation of nuclear factor-kappa B. Blood 105:3910–3917.

Vasile E, Simionescu M, Simionescu N. 1983. Visualization of the binding, endocytosis, and transcytosis of low-density lipoprotein in the arterial endothelium in situ. J Cell Biol 96:1677–1689.

Xu H, Duan J, Wang W, Dai S, Wu Y, Sun R, Ren J. 2008. Reactive oxygen species mediate oxidized low-density lipoprotein-induced endothelin-1 gene expression via extracellular signal-regulated kinase in vascular endothelial cells. J Hypertens 26:956–963.

Yin R, Dong YG, Li HL. 2006. PPARgamma phosphorylation mediated by JNK MAPK: A potential role in macrophage-derived foam cell formation. Acta Pharmacol Sin 27:1146–1152.

Zhao M, Liu Y, Wang X, New L, Han J, Brunk UT. 2002. Activation of the p38 MAP kinase pathway is required for foam cell formation from macrophages exposed to oxidized LDL. APMIS 110:458–468.

Zulli A, Buxton BF, Black MJ, Ming Z, Cameron A, Hare DL. 2006. The immunoquantification of caveolin-1 and eNOS in human and rabbit diseased blood vessels. J Histochem Cytochem 54:151–159.